A Study of Galloping Conductors on a 230 kV Transmission Line

A. S. RICHARDSON
Research Consulting Associates, 3 Wingate Road, Lexington, MA 02173 (U.S.A.)
(Received September 5, 1990)

ABSTRACT

The paper studies galloping of three-phase conductor spans on a transmission line. The spans most likely to gallop, the causes, field data, and antigallop device technologies are considered. The various remedies are ranked according to installation cost, performance, and other factors.

INTRODUCTION

A transmission line in the state of Indiana tripped, due to galloping of its three-phase conductor spans. It was locked out to prevent any further flashover and subsequent circuit breaker operation. The galloping occurred on February 14, 1990. A brief description of the line is given in Table 1. The problem of galloping transmission lines in the United States dates back over many decades, and this incident in Indiana is typical. Freezing rain and drizzle accompanied by little wind caused an ice crescent to form along the conductor span during the night. In the morning, a solid hard glaze surface had formed on the windward (west) side of the cable. The thickness of the ice was estimated at 1/8 - 1/4 in. (3 - 6 mm). The temperature was just below freezing. A few hours after sunrise the wind increased to 18 - 27 miles/h (8 - 12 m/s). The gallop was confirmed by field observation. It was reported as involving the entire line section south of Kokomo, more than 200 spans altogether.

This study was commissioned to analyze the transmission line, span by span, to identify those spans most likely to gallop again, and to study various remedies that are available to cure the problem. The scope of the study includes the theoretical basis for galloping caused by a light ice crescent, the breakdown of the likelihood of gallop, span by span, the theoretical basis for several kinds of antigallop device technologies, experimental field observation data, and a ranking of various remedies according to installation cost, performance, and other factors.

AERODYNAMICS OF THE ICE SHAPE

The question of ice shape has been studied for more than 45 years. A series of plausible shapes was studied at the National Research Council of Canada [1]. A decade later, another series of shapes was studied at MIT under contract with Edison Electrical Institute and other sponsors [2]. Still other shapes were studied at the Ontario Hydro Research Division Laboratory [3]. The most recent study of ice shapes was made in England at the Central Electricity Research Laboratory [4]. These studies used wind tunnel models, and measured the aerodynamic lift, drag, and pitching moment of coefficients as a function of the angle of attack. The Reynolds numbers for the tests have covered a wide range, from about 15 000 to 100 000. For the light ice (crescent) shape, a series of tests by Richardson and Koutselos is compared in Fig. 1. The high Reynolds number of Richardson (Re = 100 000) yields higher lift than the lower Reynolds number of Koutselos (Re = 33 000). This is in accord with previous investigations. The thickness of the crescent is not more than 10% of the basic cable diameter. By far, the thin ice shape accounts for most of the galloping conductors in the United States and in the Ontario province of Canada [5].

For the purpose of analysis, the thin ice crescent is mathematically modelled as follows:

$$C_L = -0.5 \sin(2\pi\alpha) \quad (1)$$

0378-7796/91/$3.50

TABLE 1

Transmission line characteristics
Structure properties: steel pole structures with 10 ft (3 m) davit arms, two on one side, one on the opposite side. Direct embedment in soil. Single shield wire on top of pole, spaced at a minimum of 19.6 ft (5.9 m) above top phase conductor. Electrical clearance 14 ft (4.2 m) phase to phase.

Item	American units	Si units
Conductor name	Canary	Canary
Stranding (ACSR)	54/7	54/7
Diameter	1.162 in.	29.5 mm
Weight per unit length	1.159 lb/ft	1.738 kg/m
Relative density	3240	3240
Breaking strength	31900 lb	142 kN
Conductor tension	6450 lb	28.7 kN
Torsion stiffness	907 lb ft^2/rad	370 N m^2/rad
Midspan stiffness[a]	5.2 lb ft/rad	7 N m/rad
First-mode frequency[a]	0.3 Hz	0.3 Hz
Second-mode frequency[a]	0.6 Hz	0.6 Hz

[a]These are for a 700 ft (212 m) span.

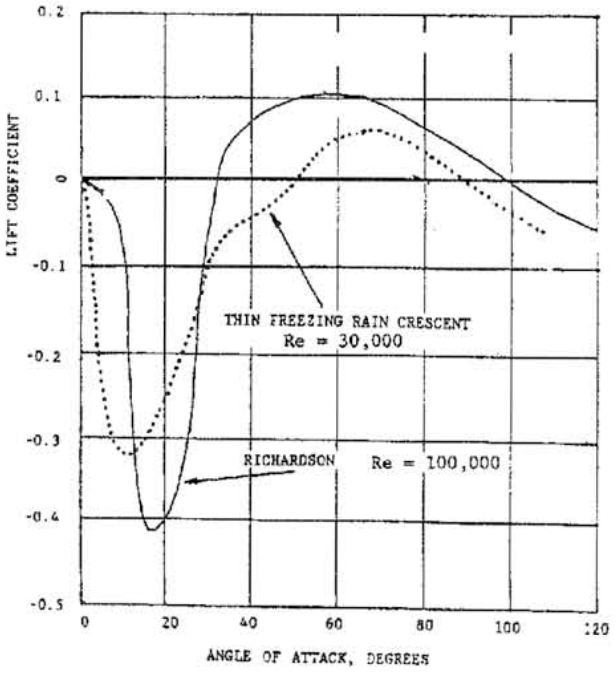

Fig. 1. Comparison of lift coefficients versus angle of attack.

The maximum lift coefficient C_L is ± 0.5, and the zero lift reversal angle, where the lift goes from negative to positive, is at an angle of attack equal to 1/2 rad, or 28.6°. This agrees closely with the experimental data of Fig. 1.

There is no perceptible aerodynamic pitching moment for the light ice shape, and the drag coefficient is a constant ($C_D = 1.0$). Throughout the study, no other ice shape is considered.

The light ice crescent is subject to Den Hartog gallop instability, according to Richardson [6, 7]. The onset of gallop is called the critical wind speed because there is no gallop below this speed; gallop builds up in proportion to the wind speed when the critical wind speed is exceeded. The value of the wind speed at this boundary is given by

$$U_c = -\omega d\mu g/(C_{La} + C_D) \qquad (2)$$

where $C_{La} + C_D < 0$ is the Den Hartog number.

In the case of the light ice shape, the Den Hartog number is -2.14.* The mechanical damping constant depends upon internal friction, joint friction, conductor tension, and temperature. The relative density is approximately equal to 3000 for ACSR-type conductors. The natural frequency is inversely proportional to the span length, directly proportional to the wave speed, axial conductor stiffness, and, in the case of dead-end poles, pole stiffness. For the line under study, there are only three dead-end poles. The remaining 185 poles are suspension type. The natural frequency for a 700 ft (212 m) span of Canary conductor, at a temperature of 30 °F (-1 °C), is 0.30 Hz. This is at a final tension of 6449 lb (28.7 kN). The natural frequency of other spans may be calculated by the inverse ratio of the other span length to this one. This is the first mode, or single-loop mode. The second mode, or two-loop mode, is just twice the first-mode frequency.

The calculation results for the first mode are plotted in Fig. 2. The critical wind speed is plotted against span identification number for a total of 190 spans. There is a band of critical wind speeds that corresponds to the range of span length. The minimum speed is 10 miles/h (4.5 m/s), while the maximum is 20 miles/h (9 m/s). The minimum span is 350 ft (106 m), while the maximum is 914 ft (277 m). The 10 miles/h corresponds to the 914 ft span, while the 20 miles/h corresponds to the 350 ft span.

The distribution of span length is seen in Fig. 3. The number of spans having length

*In all calculations herein the untwisted Den Hartog number is -1.07. This is to account for small variations of ice angle along the span.

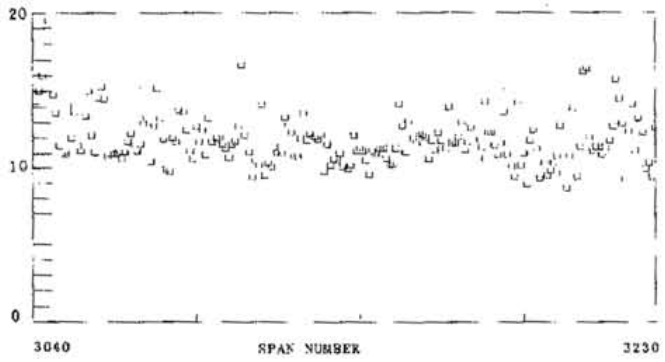

Fig. 2. Critical wind speed versus span number.

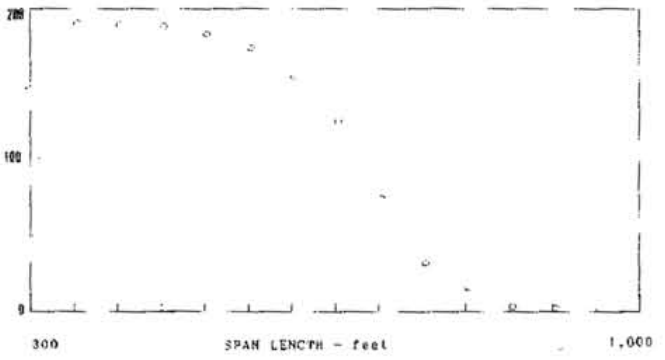

Fig. 3. Distribution of span lengths.

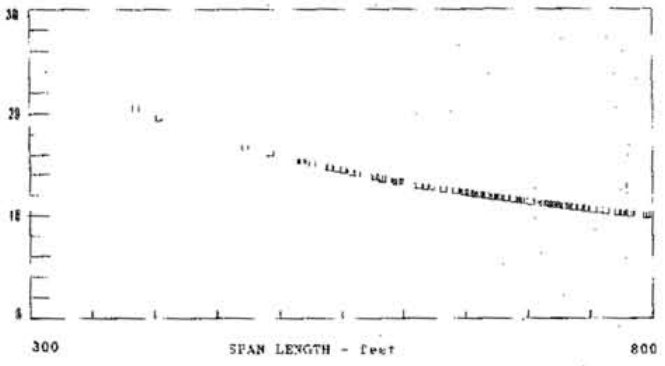

Fig. 4. Critical wind speed versus span length.

greater than the abscissa is plotted as ordinate. The median span length is about 700 ft (212 m). There are no spans greater than 914 ft (277 m).

The variation of critical wind speed with span length is illustrated in Fig. 4. The median span of 700 ft (212 m) is seen to have a critical wind speed equal to 12 miles/h (5.3 m/s). Span lengths greater than 700 ft (212 m) are estimated to have critical speeds even less than 12 miles/h. Because of the definition of critical wind speed, the gallop amplitude at the critical wind speed is zero. It is only when the wind speed exceeds the critical wind speed that the galloping takes on finite amplitude. There are no spans greater than 914 ft (277 m).

METHODS TO INCREASE THE CRITICAL WIND SPEED

Examination of eqn. (2) reveals the following possible ways to increase the critical wind speed:

(1) increase the natural frequency;
(2) increase the conductor density;
(3) increase the mechanical damping;
(4) increase the aerodynamic drag;
(5) decrease the aerodynamic lift;
(6) increase the conductor diameter.

The best way to increase the natural frequency is to increase the conductor tension. However, many conductors which gallop are already at a high tension limit for other reasons. The natural frequency could also be increased at the same tension by reducing the mass per unit length. But upon further examination of eqn. (2) it will be seen that the mass per unit length enters directly into the relative density. Hence, the critical wind speed would actually be reduced by a reduced mass per unit length.

An increased mass per unit length will have a direct effect on the wind speed, according to the equation. But, to prevent a lower frequency from accompanying such an increase, the tension must also rise in direct proportion to the mass increase. There are many practical limits to that procedure.

An increase in the mechanical damping will have a directly beneficial effect on the critical wind speed. Some practical devices are actually in use that employ that principle. For transmission lines, however, none has gone beyond the experimental stage. Operation at high voltage levels creates special problems for mechanical dampers. Also, operation can be totally defeated by ice accretion on the device itself.

Another parameter in eqn. (2) that may be altered is the Den Hartog number. This consists of two parts, the aerodynamic drag and the lift. By working on one or both, the critical wind speed may be increased. If drag only is worked on, it should be increased. If lift only is worked on, it should be decreased. There are several practical ways that these objectives can be met.

According to eqn. (2), increasing the conductor diameter should have a directly beneficial effect on the critical wind speed. However,

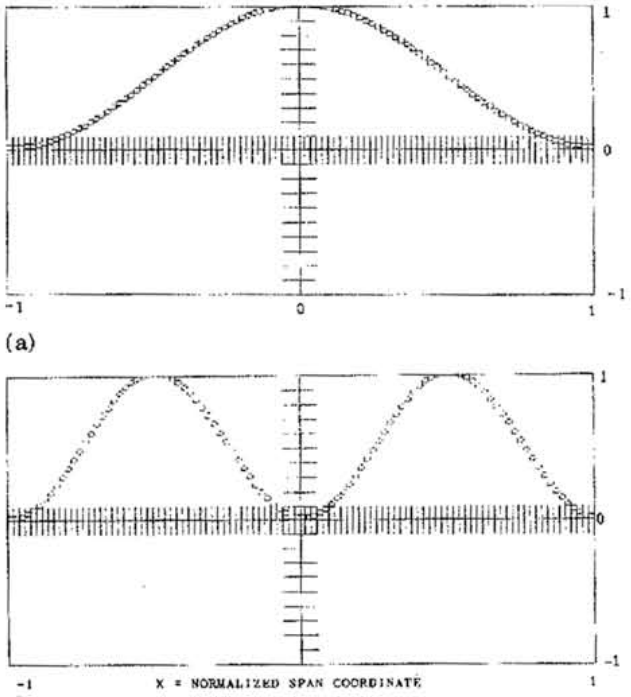

Fig. 5. Mode weighting functions: (a) first mode; (b) second mode.

the relative density parameter is inversely proportional to the square of the conductor diameter. So an increase in diameter will be counterproductive.

Some drag devices operate to increase the diameter as well, but they also cancel the lift that otherwise leads to instability. The latter effect is often more important, and more rewarding.

However, before concentrating on specific devices, it is necessary to consider spanwise effects, and the influence of finite span on the Den Hartog number.

Span effects

The mode shapes of the galloping span are illustrated in Fig. 5. The first mode is seen in Fig. 5(a) the second in Fig. 5(b). These are normal modes, so called because they are normalized to a maximum value of unity. The motion is confined within the limits set along the span. In general, at a wind speed above critical for both modes, there will be evidence of each kind of motion in a single span. If the wind speed is above the first-mode critical, but below the second-mode critical, there will be only the first-mode motion. Sometimes, on dead-end spans, the two natural frequencies are nearly equal, and both modes will be present. The first-mode shape will be different from that seen in Fig. 5(a) for such a case. It has been proved that the mode shapes do not alter the critical wind speed *per se*, if the Den Hartog number is constant along the span [2]. Later it was proved that the variation of Den Hartog number due to twisting along the conductor does increase the critical wind speed [8].

In other words, while mode shape itself cannot be controlled, its effect on the critical wind speed can be calculated when something else is used to vary the Den Hartog number along the span.

First, consider the effect that the mode shape has on the overall span stability coefficient [8]:

$$\mathrm{Ca}_1 = \int_{-1}^{1} \mathrm{Ca}(x) \cos^2(\pi x/2)\, dx \tag{3}$$

$$\mathrm{Ca}_2 = \int_{1}^{1} \mathrm{Ca}(x) \sin^2(\pi x)\, dx \tag{4}$$

where Ca_1 and Ca_2 are the first- and second-mode span-weighted Den Hartog numbers, respectively, $\mathrm{Ca}(x)$ is the spanwise variation of the Den Hartog number, and x is the dummy variable of integration along the span.

The first kind of gallop remedy is the increase of aerodynamic drag. This may be apportioned along the span so as to combat the negative Den Hartog number. But any drag increase will also develop more loading of the line support structure. Hence, it is of interest to find the optimum apportioning of drag on the span. Some clues concerning this procedure are found in the way the mode weight functions act. For example, a certain strategy for allocating drag to maximize the effect for the first mode will not work very well for the second-mode gallop. The reverse is also true. The amount of added drag is also an important factor. One does not just go out and plaster the line with more drag. A scientific approach is required.

The contribution of the mode weighting over the interval of drag treatment as a function of treatment interval and location is seen in Table 2. A 33% span treatment centered at the midspan yields a contribution of about 61% for the first mode, but only about 20% for the second mode. This scheme would have little effect on the second-mode gallop. If the

TABLE 2

Fractional contribution to mode-shape integrals

First mode	Second mode	Integration parameters[a]
	Cover factor 33%	
0.610	0.197	$b = 0$ $A = -0.33$ $B = 0.33$
0.475	0.401	$b = 0.33$ $A = 0$ $B = 0.66$
	Cover factor 50%	
0.823	0.510	$b = 0$ $A = -0.50$ $B = 0.50$
0.677	0.502	$b = 0.33$ $A = -0.17$ $B = 0.83$

[a] b is the center of the treatment range (fraction of semispan length); midspan is 0%, 1/3 span point is 33%; A is the lower integration limit; B is the upper integration limit; the span coordinate runs from + 1 to −1.

same 33% span treatment is centered at the 1/3 span point, it produces comparable contributions for each mode. Higher cover factors produce larger contributions. A 50% cover factor produces about equal contributions for each mode when the drag treatment is centered at the 25% span point (not shown).

The diameter of the drag treatment body also enters into the equation. A lower span cover factor is required with a larger drag body. An illustration of this effect is seen in Table 3. This Table shows the increase in the critical wind speed as a percentage. Substantial increases in the critical wind speed are possible for both modes.

Effect of twisting

Another way to alter the aerodynamic properties of the span is by adding a device that causes the span to twist. The Den Hartog number corresponding to a twist angle Q is obtained from

$$\mathrm{Ca} = -\pi \cos(2\pi Q) + C_D \qquad (5)$$

This is based on the analytic model of the ice shape, eqn. (1).

A twist angle of 11° is all that is required to eliminate gallop altogether, and a twist angle of only 9° will increase the critical wind speed by 200%.

There are devices that will twist the conductor. Some of these are operated by aerodynamic pitching moments, while others are operated by inertia or acceleration. Depending on where the devices are located in the span, the twist will be symmetrical about the midspan, or unsymmetrical.

The mode weighting functions for a constant Den Hartog number (zero twist) are illustrated in Fig. 5. The area under these curves is expressed by eqns. (3) and (4), but multiplied by the Den Hartog number. When the number is negative, the area is negative and the critical wind speed may be found from eqn. (2). The smaller the negative area, the larger the critical wind speed. As already stated, twisting causes the Den Hartog number to become more positive, reducing its numerical value, and thereby increasing the critical wind speed. A symmetrical twist of 15° produces a stable span (no gallop), as observed in Fig. 6.

The first mode is totally stable, while the second mode still has a small negative net area, but it corresponds to a very high critical wind speed. A 15° symmetrical twist, approximating a cosine curve, could be produced by two units located at each of the 1/3 span points.

TABLE 3

Increase of critical wind speed due to drag-only devices (Den Hartog number = −2, drag device $C_D = 2.0$[a])

Span cover (%)	Span location[b] (%)	Increase in critical wind speed (%)
10	0	71
10	33	46
20	0	381
20	33	153
30	0	No gallop
30	33	701

[a] The $C_D = 2$ is a drag device having twice the conductor diameter.

[b] Midspan is 0%, 1/3 span point is 33%.

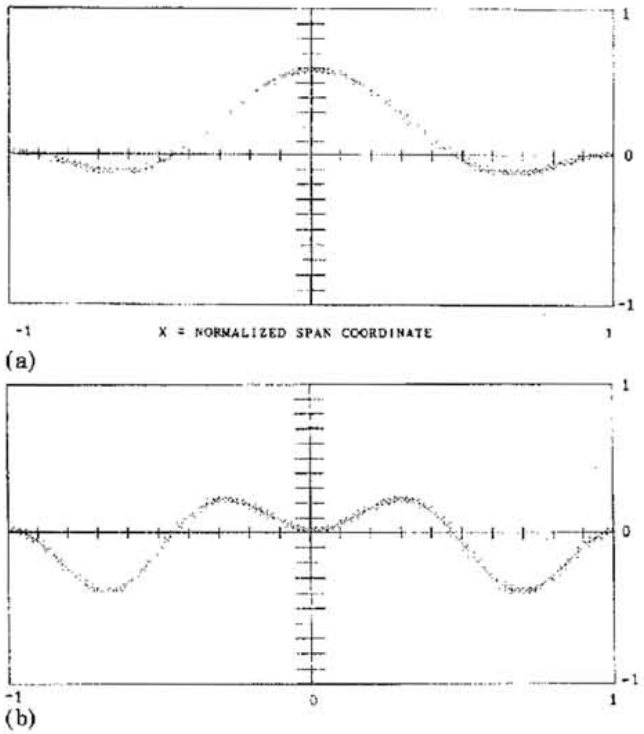

Fig. 6. Den Hartog number for a 15° twist: (a) first mode; (b) second mode.

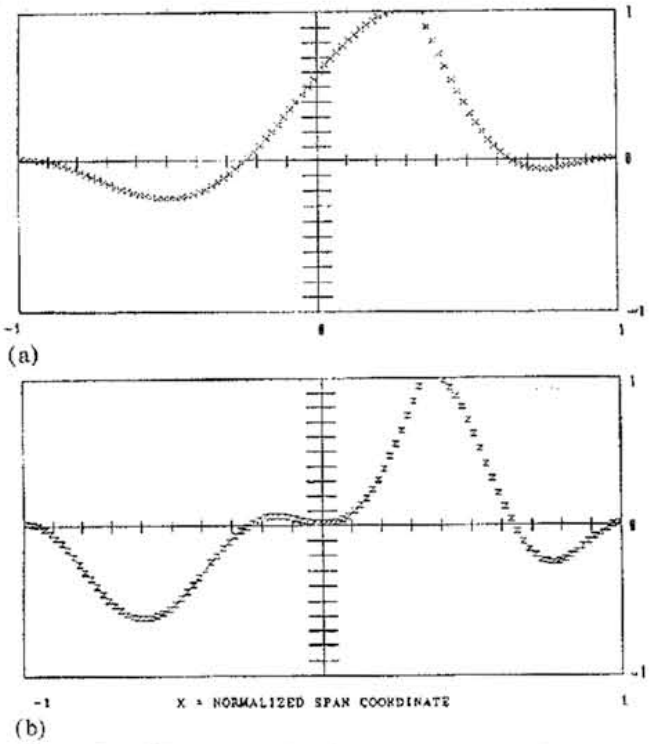

Fig. 8. Den Hartog number for a 20° twist; (a) first mode; (b) second mode.

In each of these Figures the maximum ordinate scale is unity. This is obtained by normalizing the local (weighted) Den Hartog number due to local twist to the untwisted Den Hartog number.

Rather than using two devices in a span, it is more economical to use only one twisting device, located at the 1/3 span point. This will develop an unsymmetrical twist along the span.

The analysis of such a case for a 10° maximum twist at the 1/3 span point is seen in Fig. 7. The negative area has been reduced, indicating an increase of critical wind speed (by nearly a factor of two).

Increasing the twist to 20° produces a stable span, both in the first mode and in the second mode. The net area is positive, as seen in Fig. 8. The local Den Hartog numbers are clearly influenced by both mode shape and twist angle. The greatest influence (toward stability) is at the 1/3 span point, where the twist is the maximum. In the second mode there is no motion at midspan, hence no value for the integrand. The first and second modes can be made stable, or, if not stable, the critical wind speeds can be increased several times.

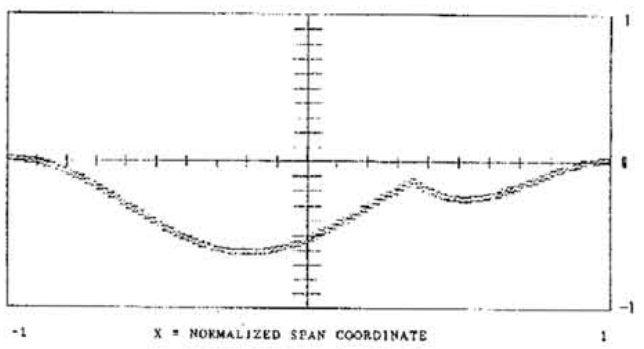

Fig. 7. Den Hartog number for a 10° twist: first mode, unsymmetrical twist.

The twisting affects the third mode as well, as seen in Fig. 9. The 15° twist is insufficient to cause stability, but only enough to increase the critical wind speed by a factor of more than two. This is sufficient for practical purposes because the untwisted critical wind speed for the third mode is three times the untwisted critical wind speed for the first mode. A 20° twist angle improves the situation even more (Fig. 9(b)).

Twisting, either by symmetrical or unsymmetrical means, increases the critical wind speed by several hundred percent, and can eliminate galloping altogether.

GALLOP AMPLITUDE

The linear theory is not able to predict the gallop amplitude. A nonlinear theory, based

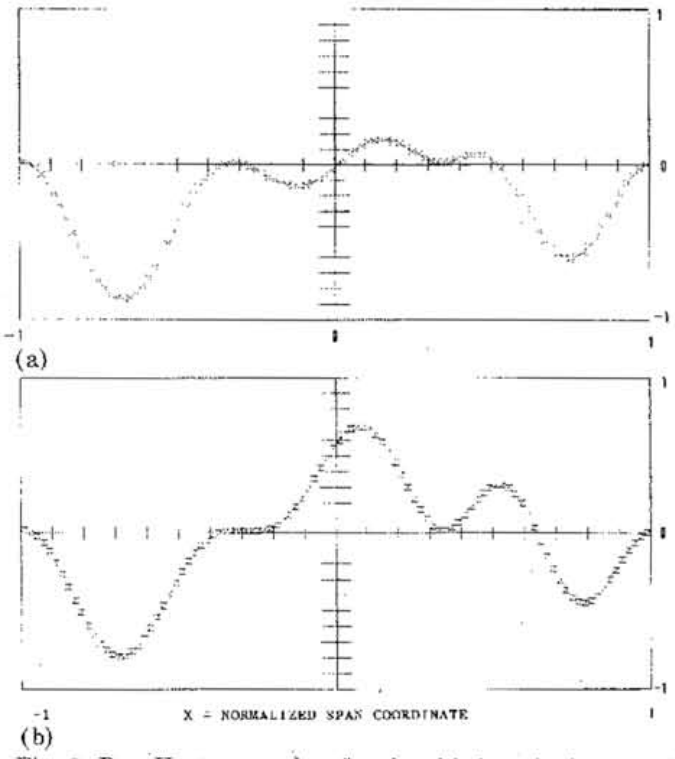

Fig. 9. Den Hartog number for the third mode due to (a) a 15° twist, and (b) a 20° twist.

on the balance of energy between the aerodynamic and mechanical damping forces, can predict the gallop amplitude [6, 7]. The analysis shows a gradual buildup of the dynamic angle of attack due to the gallop motion:

$$a = \omega Y/U \tag{6}$$

The angle of attack buildup may be approximated by the formula

$$a = (2/\pi)a_0 \cos^{-1}(U_c/U) \tag{7}$$

This is a simple expression to be used for any lift reversal angle a_0, any critical wind speed U_c, and any maximum lift coefficient. The only requirement is that the form of the lift curve must be a sine curve as approximated here in eqn. (1). In that expression $a_0 = 0.5$, and the maximum lift coefficient is -0.5.

Combining eqns. (5) and (6), the gallop amplitude is calculated. For the range of span lengths from 300 ft (91 m) to 800 ft (242 m), the angle of attack is plotted in Fig. 10 for two different wind speeds, 20 and 35 miles/h (9 and 15 m/s). The maximum possible angle of attack is 0.5 rad. The Figure indicates that most spans are within 80% of that figure at both wind speeds.

The above equations have been combined with eqn. (2) to obtain a picture of galloping over the entire line at wind speeds of 20 and 35 miles/h (9 and 15 m/s) (Fig. 11). According

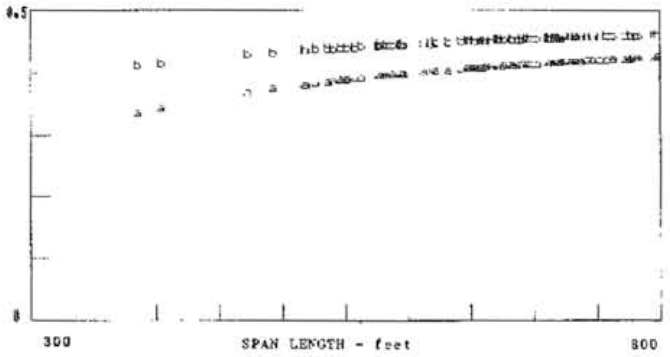

Fig. 10. Angle of attack versus span length for wind speeds of 20 miles/h (9 m/s) (curve a), and 35 miles/h (15 m/s) (curve b).

to Table 1, the flashover double amplitude is 14 ft (4 m). At 20 miles/h there is only one flashover predicted, but at 35 miles/h only seven spans will not have flashed. This is a clear indication that a serious gallop problem exists on this transmission line. Further, a separate study was made on the three dead-end spans, and, while the gallop amplitude is smaller, there is sufficient risk to consider protective measures for these as well.

It is obvious from eqns. (2) and (6) that the natural frequency of the span plays a dominant role in both critical wind speed and gallop amplitude. The variation of the natural frequency, in units of cycles per minute, was

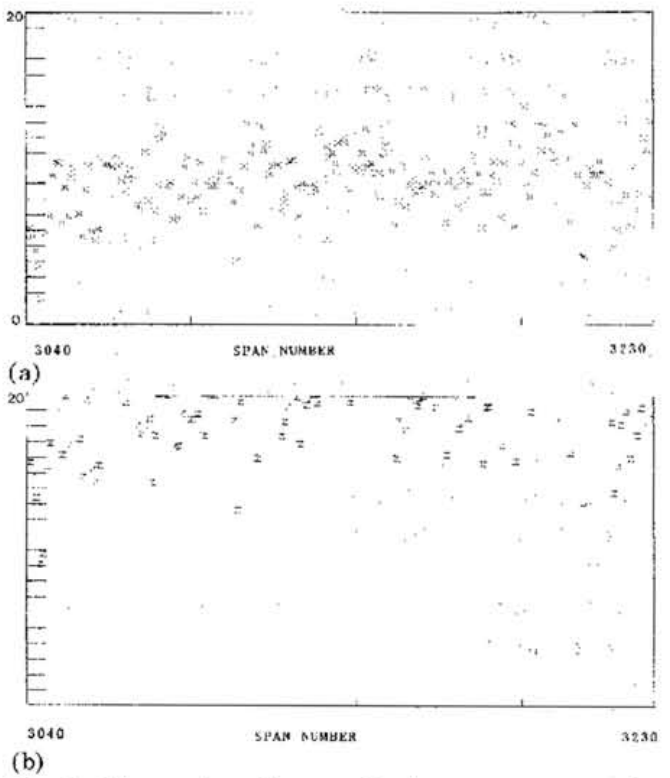

Fig. 11. First-mode gallop amplitude versus span number for wind speeds of (a) 20 miles/h (9 m/s) and (b) 35 miles/h (15 m/s).

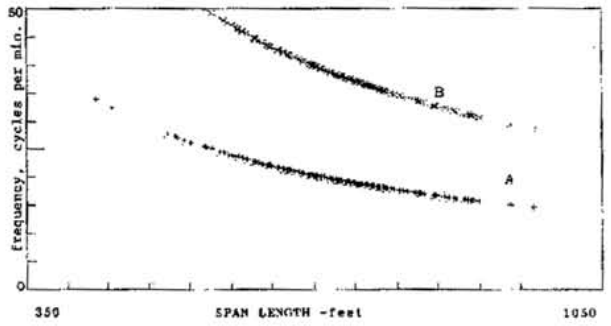

Fig. 12. Frequency of gallop versus span length: curve A, first mode; curve B, second mode.

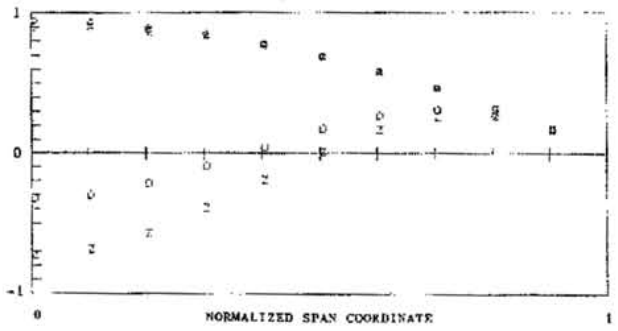

Fig. 13. Energy input function (semispan): low drag (o, O); high drag (x, Z).

calculated as a function of span length for both the first and second modes (Fig. 12). The method used employed the so-called string modes because it was shown some time ago that suspended spans on long insulators may be closely approximated by string modes, in the case of the first two gallop modes. Even for the dead-end spans here, the same string modes are used because these dead-end spans are not double-ended, but only single-ended.

DAMPING REQUIRED TO LIMIT AMPLITUDE

After the critical wind speed is exceeded, the gallop amplitude builds up as the wind speed increases above critical. The previous Section has demonstrated that both twisting of the conductor span and augmentation of the aerodynamic drag have a beneficial effect on the critical wind speed, that is, it is increased. It is also of interest to see how these two effects influence the amplitude buildup. The method used to assess that influence is to calculate levels of mechanical damping that would be required to balance the aerodynamic energy due to gallop motion at prescribed amplitudes. In other words, for a fixed amplitude of gallop, how does the required mechanical damping change as either drag or twist is added?

A review of the nonlinear theory [6, 7] reveals the following equation:

$$E/qAY = -S_1(J_0 - J_2) - 2C_D J_1 \tag{8}$$

and

$$S_1 = -2A_m J_1(\pi a/a_0) \tag{9}$$

When a twist angle b occurs, the describing function is modified:

$$S_1^* = \cos(\pi b/a_0)\, S_1 \tag{10}$$

This was obtained by Fourier series analysis according to Fante [9].

These equations are used to estimate the mechanical damping required to establish equilibrium of energy between the aerodynamic input and the energy dissipated by damping. They are applicable to a member that is galloping with constant amplitude along the span.

In a transmission line, the amplitude follows a cosine (first-mode) or a sine (second-mode) wave. The above equations apply to those cases as well, but the amplitude must be adjusted to follow the particular mode shape. The resulting energy for the whole span is found by integration point by point along the span.

An illustration of this process is seen in Fig. 13. Only half a span is shown in the Figure because the mode is symmetric about the midspan. The dimensionless energy levels according to eqn. (8) are seen to follow the mode shape for small gallop amplitude (points labelled o and x). The dimensionless energy levels are distorted for large gallop amplitude (points labelled O and Z). In the former case, the gallop amplitude at the midspan is $a = 0.05$, while in the latter case, the amplitude is $a = 0.5$. The difference between the labels o and x is that, in the former, the drag coefficient is equal to unity along the span, while in the latter it is equal to 1.5. Increasing the drag coefficient has little effect on the energy input from the wind at low gallop amplitude.

The difference between the curves labelled O and Z is the same, that is, the points refer to

$C_D = 1.0$ and 1.5, respectively. The larger drag develops more net negative area under the curve, thus providing less wind energy input, and requiring less mechanical damping.

To find the numerical value of the wind energy input,

$$E/qAY = -a(C_{La} + C_D)_0 \int_{-1}^{1} F[a, x]\, dx \qquad (11)$$

where $(C_{La} + C_D)_0$ is the Den Hartog number at zero angle of attack, and $F[a, x]$ is a span function based on eqn. (8).

In the present illustrative example, the function $F[a, x]$ is shown only for half a span. It is the result obtained by dividing the point-by-point calculation of eqn. (8) by the numerical value of $a(C_{La} + C_D)$.

This procedure may be applied to find the best distribution of drag on the span for a particular ice-shape model. Here, the model is light ice.

An illustration of the effect of twisting is seen in Fig. 14. The curve labelled u is for $a = 0.05$ (small amplitude). This is the same as the curve labelled o in the previous Figure, $C_D = 1$. The curves labelled z and o in Fig. 14 are for a twist angle of 20° at midspan. The label z is for small amplitude ($a = 0.05$), while the label o is for large amplitude ($a = 0.5$). Comparison of the two Figures clearly shows that twisting reduces the wind energy input at both low and high amplitudes, while drag increases are effective only at high amplitudes.

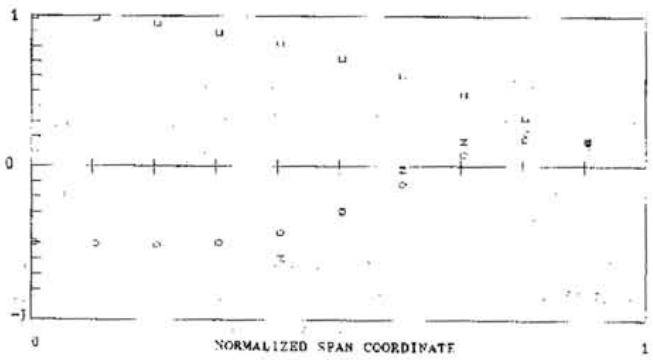

Fig. 14. Energy input parameter (semispan): 0° twist (u); 20° twist (o, z).

REMEDIES

The configuration of steel pole structures creates a risk of conductor flashover on the side having two phases separated by a 14 ft (4 m) vertical clearance. The remaining phase is on the other side of the steel pole, so gallop on that phase will not create phase-to-phase flashover. The static wire is on top of the pole, and it is unlikely to gallop into the conductor top phase. Hence, a suitable solution to the problem will involve antigallop treatment of the two phases on one side of the pole.

The following commercially available antigallop devices are considered: Windamper, PLP Air Flow Spoiler, AR Spoiler, AR Twister, detuning pendulum. These are listed in Table 4. The various devices are described in the Appendix.

TABLE 4

Relative rating of antigallop devices[a]

	Windamper	PLP Spoiler	AR Spoiler	AR Twister
Drag device	No	Yes	Yes	No
Twist device	Yes	No	Yes	Yes
Increased drag	< 2%	25% - 40%	15% - 25%	< 1%
EHV use	Yes	No	No	Yes
Material	Aluminum	Plastic	Plastic	Aluminum
Weight	22 lb	1.2 lb/ft	0.5 lb/ft	12 lb
Length	4 ft	14 ft	10 ft	1 ft
Material cost	US $185	US $22	US $15	US $95
Delivery time	6 weeks	?	2 weeks	3 weeks
Installed cost (on 700 ft span)	US $225	US $560	US $315	US $125

[a]Because the detuning pendulum is not effective for the Den Hartog type of gallop, it is not considered here as a remedy. However, it is described in the Appendix.

PERFORMANCE

The performance data for the devices are sketchy. No uniform method has been found to present the data. Thus, it is not possible to study performance, except in a few cases [10-12]. Quantitative data are particularly difficult to obtain. Much of the data already published have been self-serving for the detuning pendulum advocates [13-15]. A rather complicated three-dimensional scheme has been devised to present data on a normalized amplitude basis. The problem with this method is that the raw data are couched in the presentation methodology, permitting no independent assessment by the reader. Conclusions are drawn about performances that are impossible to verify.

In the present situation, a gallop amplitude of 14 ft (± 7 ft or ± 2.1 m) will cause flashover. A gallop control device that works to control gallop to less than 5 ft (± 2.5 ft or ± 0.75 m) is expected to solve the present problem. Vendors of antigallop devices should be prepared to guarantee gallop control to less than 5 ft peak-to-peak. Otherwise, the device is not worth installing.

An illustration of the type of data that should be provided is presented in Tables 5 and 6.

The Pass/Fail scheme leaves no doubt in the reader's mind concerning the gallop amplitude (Table 5). When two devices are compared the Pass/Fail numbers for each may be used to assess the performance. The placebo data are very important, if available. This is a means of ranking those spans which galloped (or not), but which had no antigallop device treatment (Table 6). Placebos are formed from observations in single-, double-, and triple-circuit lines, where only one device per phase is installed. The remaining phases serve as placebos. Comparing one placebo against another in the same span yields Pass/Fail data for the placebo. Unless the device Pass/Fail ratio is significantly larger the device is concluded to be no better than the placebo.

A performance index can be established:

$$\mathrm{PI} = \frac{[\mathrm{Pass/Fail}]\mathrm{device}}{[\mathrm{Pass/Fail}]\mathrm{placebo}} \tag{12}$$

For the Windamper device,

$$\mathrm{PI} = \frac{38/1}{53/152} = 109$$

For the detuner device,

$$\mathrm{PI} = \frac{20/16}{158/149} = 1.18$$

TABLE 5

Comparison between the detuner and the Windamper

Data source		Detuner		
		Pass[a]	Fail[a]	Total
U.S. gallop data 1978, 1979, 1980 [5]		8	5	13
Ontario Hydro data 1977, 1978, 1979, 1980 [5]		12	11	23
	Total	20	16	36
Data Source		Windamper		
		Pass[a]	Fail[a]	Total
Ontario Hydro data 1977, 1978, 1979 [16]		38	1	39

[a]Pass: gallop amplitude of reference spans more than 5 ft, that of control spans less than 5 ft (1.5 m). Fail: gallop amplitude of control spans more than 5 ft.

TABLE 6

Comparison of the placebo data[a] for the detuner and the Windamper

Data source		Detuner		
		Pass[b]	Fail[b]	Total
U.S. gallop data 1978, 1979, 1980 [5]		11	34	45
Ontario Hydro data 1977, 1978, 1979, 1980 [5]		147	115	262
	Total	158	149	307
Data source		Windamper		
		Pass[b]	Fail[b]	Total
Ontario Hydro data 1977, 1978, 1979 [18]		53	152	205

[a]Placebo data are formed from an untreated span and compared with all other reference spans, assuming the untreated span controls gallop. The Pass/Fail ratio for the placebo may be compared with the Pass/Fail ratio for the device to obtain the effectiveness or performance figure of merit. The device ratio should be several times the placebo ratio.

[b]Pass: gallop amplitude of reference spans more than 5 ft, control spans less than 5 ft (1.5 m). Fail: gallop amplitude of control spans more than 5 ft.

The conclusions reached in this example are (1) the Windamper is 109 times more effective than its placebo, the detuner is 1.18 times more effective than its placebo, and (3) the ratio between the two PIs is 92:1. In 90% of the observations the ice thickness was less than 1/8 in. The type of comparison illustrated here is based on well-established statistical sampling techniques, and in particular has been used in the medical field to evaluate the effect of drugs.

CONCLUSIONS

The study has shown that the transmission line is vulnerable to gallop motion, and flashover at wind speeds of 20 miles/h (8.9 m/s) and higher.

The use of (1) drag enhancement devices or (2) conductor twisting devices is predicted to prevent flashover.

The use of detuning pendulums is predicted not to prevent flashover.

ACKNOWLEDGEMENT

Transmission line protective technologies, and in particular advanced production prototypes of the 'Twister Galloping Indicator and Galloping Preventor' devices, are now being field tested in a three-year project financed by the U.S. Department of Energy under Grant No. DE-FG01-90CE15429 to Research Consulting Associates, Inc.

NOMENCLATURE

A	= span × diameter, reference area
A_m	maximum lift coefficient
a	$=\omega Y/U$, peak dynamic angle of attack
a_0	zero lift reversal angle
b	local twist angle
Ca	Den Hartog number
Ca_1	Den Hartog number, first mode
Ca_2	Den Hartog number, second mode
C_D	drag coefficient
C_L	lift coefficient
$C_{L,a}$	slope of lift coefficient
d	conductor diameter
E	energy input (per cycle) from the wind
$F[\ ]$	span function based on eqn. (8)
g	mechanical damping loss factor
J_0	zeroth-order Bessel function of first kind
J_1	first-order Bessel function of first kind
J_2	second-order Bessel function of first kind
m	conductor mass per unit length
Q	twist angle
q	$=\rho U^2/2$, dynamic wind pressure
S_1	lift describing function
S_1^*	describing function with twist
U	wind speed
U_c	critical wind speed
x	span coordinate, normalized to semi-span
Y	maximum peak gallop amplitude
α	angle of attack
ρ	air density
μ	$=m/(\rho d^2/2)$, relative density
ω	natural frequency, rad/s

REFERENCES

1 F. Cheers, A note on galloping conductors, *Rep. No. MT-14*, Nat. Res. Counc. Can., June 1950.
2 A. S. Richardson, J. R. Martuccelli and W. S. Price, Research study of galloping of electric power transmission lines, *Wind Effects on Bridges and Structures*, Vol II, Nat. Phys. Lab., Teddington, U.K., 1963, p. 613.
3 J. Chadha, Detailed measurements of aerodynamic forces acting on iced conductors, *Rep. No. 73-254-K*, Ontario Hydro Res. Div., Toronto, Canada, 1973.
4 L. T. Koutselos and M. J. Tunstall, Further studies of the galloping instability of natural ice accretions on overhead line conductors, *4th Int. Conf. Atmospheric Icing of Structures, Paris, 1988*, Paper A9.1.
5 D. G. Havard, Galloping control by detuning, progress report no. 2, *EPRI Project No. RP-1095*, Ontario Hydro Res. Div., Toronto, Canada, 1981.
6 A. S. Richardson, Predicting galloping amplitudes—I, *ASCE J. Eng. Mech., 112* (1986) 1723.
7 A. S. Richardson, Predicting galloping amplitudes—II, *ASCE J. Eng. Mech., 114* (1988) 1945.
8 A. S. Richardson, Some effects of twisting on galloping conductors, *IEEE Trans., PAS-99* (1980) 811.
9 R. L. Fante, *Signal Analysis and Estimation, an Introduction*, Wiley, New York, 1988, p. 4.
10 A. S. Richardson, Binary statistics of galloping observations, *ASCE J. Struct. Eng., 112* (1986) 1957.
11 D. G. Havard, Binary statistics of galloping observations, Discussion, *ASCE J. Struct. Eng., 114* (1988) 2150.
12 D. G. Havard and C. J. Pon, Galloping conductor control—status 1988, *4th Int. Conf. Atmospheric Icing of Structures, Paris, 1988*, Paper B6.1.
13 D. G. Havard, Control of galloping conductors by detuning, *Proc. CIGRE, 1980*, Paper No. 22-05.

14 D. G. Havard, Galloping control by detuning, progress report no. 4, *EPRI Project No. RP-1095*, Ontario Hydro Res. Div., Toronto, Canada, 1982.
15 D. G. Havard, The economic benefits of galloping controls, *Proc. CIGRE, 1982*, Paper No. 22-02.
16 R. G. Ko, Performance of the modified drag damper as a galloping control device for single conductors, *Rep. No. 80-270-H*, Ontario Hydro Res. Div., Toronto, Canada, 1980.

APPENDIX

Antigallop devices

The antigallop devices discussed in the text are described more fully here. First, a general description of the physical characteristics is given, and then a brief description of the operating principle. When patents have been issued, they are cited.

Windamper

The Windamper is comprised of two back-to-back panels of sheet metal (usually aluminum) shaped in the form of an elongated channel. It is arranged to hang below the conductor as in a rigid suspension from two clamps attached to the conductor. The top of the unit is wider than the bottom. Corona rings are used at EHV voltages above 230 kV.

When ice forms, it takes on a characteristic shape pattern facing into the wind. A crescent shape is formed along the windward side of the conductor. This is an unstable ice shape. When wind speed increases to the critical wind speed and beyond, the Windamper causes the conductor to twist, thereby altering the lift and diminishing the maximum possible gallop amplitude. Patents have been issued in the United States (3,440,328), Canada (725,621), Germany (1.812,644), Belgium (725,601), The Netherlands (157,756), Switzerland (483,140) and the United Kingdom (1,246,310).

PLP spoiler

The PLP spoiler is formed from a 14 ft (4.2 m) length of plastic rod about equal to the diameter of the conductor. It has special grips at each end to hold it to the conductor after being wrapped around several times.

The device is designed to alter the formation of ice on the conductor and to create drag in place of lift. A patent has been issued in the United States (4,420,059).

AR spoiler

The AR spoiler is formed from lengths of plastic tubing about 2 in. (52 mm) in diameter, and 10 ft (3 m) in length. It is attached to the underside of the conductor by lashing rods, according to a prescribed distribution.

The underside location of the device insures a high drag component to increase the critical wind speed for gallop. At higher wind speeds the units cause the conductor to twist, creating changes in the lift pattern (similar to the Windamper principle).

AR twister

The AR twister is designed to be installed at the 33% - 40% span location. It is installed initially upside down. Gravity causes it to twist the conductor up to an angle of 140°. The unit is all aluminum and is mounted by a single bolt clamp. The size of the unit depends upon the conductor size and span length. A United States patent has been issued (4,777,327).

When ice forms along the windward side of the conductor and a condition of gallop is reached, the action of the gallop itself sets the AR twister into motion. The twisting motion results from the cancellation of gravity, causing the AR twister to seek an equilibrium position close to its initial (upside-down) orientation. This action twists the ice all along the conductor span, modulating the lift, and returning the conductor to a stable configuration.

Detuning pendulum

The detuning pendulum is a heavy weight mounted in a vertical plane so that the twisting motion of the conductor is prevented. It is placed at several points along the span (usually four).

The detuning pendulum alters the torsional frequency of the conductor span. It has no effect on Den Hartog type gallop. It may be effective for some forms of bundle conductor gallop.

Recommendations

The foregoing analysis has demonstrated the beneficial effects of (1) increased drag and (2) twisting. The latter effects are more powerful, and do not carry a large penalty, such as increased structure loading.

The device that has the greatest field experience (over twenty years), with no negative side-effects reported, is the Windamper. Performance data prove that large amplitudes of gallop are eliminated. Other devices have some residual gallop left over.

It is recommended that the transmission line be equipped with Windampers and twisters over its entire length —a total of about 200 spans.